Spectral discrimination of color input devices

***Peter Morovič**[*] **and Ján Morovič**[**]*

[*] ***Research Center for Frontier Medical Engineering, Chiba University, Japan***

[**] ***Hewlett–Packard Company, Spain***

Abstract

The ability to record different signals when imaging surfaces of differing spectral properties is a pre-requisite for being able to reconstruct spectra from data captured by a color imaging device. The question of which spectral differences can be discriminated between by a given input color imaging device is therefore addressed here by sampling the space of all possible surface spectral reflectances, simulating a device's response to the samples and then identifying regions in which discrimination is possible. Results of applying the technique to the model of an actual and a theoretical, narrow-band camera are also shown to illustrate the information provided by the approach presented here.

Introduction

An input imaging device, such as a digital camera or scanner, records a signal in response to the electromagnetic radiation that is incident on its sensor. As a consequence the device can be judged from at least three perspectives: First, how well an object's color can be predicted from a recorded signal. Second, how well the object's spectral reflectance or transmittance can be predicted. Third, whether the signals recorded for two objects that have different spectral properties will also be different. The first and second perspectives have been addressed in the color correction and spectral reconstruction literature[18, 8] and the third will be the subject of the present paper. More specifically the question we ask here is, which of the possible spectral differences will result in different signals being recorded by a given input imaging device.

The space of all possible surface spectral reflectances is the Object Color Solid [15] and it will be the recording of differences in this space that will be considered here. Assuming q samples of the electromagnetic spectrum's visible range are used to represent spectral functions, this space can be defined as a hyper–cube in $\mathbb{R}^q$. The faces of this cube are planes along 0 and 1 in each of the q dimensions and each point in this hyper–cube corresponds to a physically possible surface that reflects no less than no light and no more than all light.

Digital color input devices record a sampling of the color signal (e.g., light reflected, transmitted or emitted by an object) incident on their sensors through color filters. In trichromatic devices these filters generally correspond to red, green and blue, however more recently devices with c ($3 \ll c \ll q$) channels have been developed and successfully used(e.g. [3]). For reflective and transmissive objects, color image acquisition is therefore a mapping from a hyper–cube in $\mathbb{R}^q$ to a body of color responses, in $\mathbb{R}^c$. Since $c \ll q$ this mapping is also a lossy compression in that multiple surface reflectances or transmittances induce the same response – a phenomenon known as metamerism.

In the process of image acquisition a number of factors other than a device's sensors and filters affect the recorded signal, such as the linearity of the device (dynamic response function – DRF), the number of bits used to encode the signal (quantization bit–depth) and the differences that can be observed when repeating the same image capture (repeatability threshold).

In this paper input color imaging devices are examined from the point of view of how the process of color image formation, from surface reflectances in $\mathbb{R}^q$ to device responses in $\mathbb{R}^c$, affects the recording of differences in the OCS. In particular we will study the effect of the acquisition process on the OCS' volume in $\mathbb{R}^q$ by computing that sub–set of the OCS in which a device is able to discriminate locally between differences.

In order to address this problem it is necessary to sample the entire space of possible surface spectral reflectances, i.e., the hyper-cube in $\mathbb{R}^q$, that form the set of possible surface stimuli to an input color imaging device. Given this sampling, it is then possible to determine the range across which differences in stimuli can be sensed by a device.

Sampling a q-dimensional hyper-cube of surface spectral reflectances is however computationally prohibitive. The number of extreme vertices alone of this hyper-cube is 2^q, which for a sampling of $q = 31$ ($10nm$ steps between $400nm$ and $700nm$) is 2.2×10^9. Of course examining these vertices alone is not sufficient in order to determine the range of discriminability of a device and a much finer sampling is necessary.

Previously, a similar problem was addressed[11] by determining the sub–space of the OCS in the CIE L*a*b* color space in which a device is able to discriminate and this has also been attempted in two other cases [14, 5]. The novelty of the current approach is in addressing the problem directly in the space of surface spectral reflectances, thus resulting in a boundary descriptor that is not subject to metamerism.

The paper is organized as follows. First considerations about the OCS and it's useful definition using a linear model representation are laid out. Then a color image formation model of an input device is described. Given the OCS and the model of color formation, the method to compute the sub-set of OCS in which the device can discriminate is presented. Finally examples are given of applying the current approach to a standard RGB device and a theoretical device with narrow band sensors.

The object color solid

The Object Color Solid is the set of physically possible surface spectral reflectances, whereby physical possibility constrains reflectances to be non-negative (no less than no light is reflected by each surface) and less than or equal to one (no more than all

light is reflected by each surface)[1]. Assuming reflectances are represented as $q \times 1$ vectors $\mathbf{r}$, the OCS is a hypercube in $\mathbb{R}^q$ with 2^q vertices defined by the $2q$ inequalities:

$$\begin{aligned} \mathbf{r} &\geq \mathbf{0} \\ \mathbf{r} &\leq \mathbf{1} \end{aligned} \tag{1}$$

where $\mathbf{0}$ and $\mathbf{1}$ are $q \times 1$ vectors of zeros and ones respectively.

It is common to represent surface reflectance vectors as uniformly sampled vectors at q wavelengths within the visible range. The sampling parameter q however, depends on factors such as measurement device precision and representation capabilities rather than actual dimensionality of surface spectral reflectances. In fact, it has been found that surface spectral reflectances can be well represented within a linear model basis[7], derived by means of statistical data analysis tools such as Principal Component Analysis (PCA) [9].

Let $\mathbf{B}$ be the $q \times d$ matrix of basis vectors, defining the axes of a new, d–dimensional space relative to the existing q–dimensional realm. A $q \times 1$ reflectance vector $\mathbf{r}$ can be represented within the basis $\mathbf{B}$ as:

$$\mathbf{r} \approx \mathbf{B}\mathbf{w} \tag{2}$$

where $\mathbf{w}$ is a $d \times 1$ vector corresponding to the reflectance $\mathbf{r}$. The degree to which Eq. (2) is an approximation depends on how well $\mathbf{B}$ represents the space of $\mathbf{r}$.

Given a set of surface spectral reflectances, the best d dimensional basis (in the sense of L2 Euclidean distance between original and representation) is found by means of PCA. This method simply solves for axes of maximum variance in the data. In general, the more bases are employed for the representation, the better the approximation. However, there is a limit to the number of useful principal components. If the analyzed data is truly d dimensional (i.e. there exists a d dimensional basis within which it can be represented without error), then the approximation in Eq. (2) becomes an equality and no improvement is achieved beyond the d–th basis, assuming these are optimal.

In Table (1) the accuracy of a linear model representation is examined. PCA was performed on a set of 2086 surface spectral reflectances comprising paper samples (the Macbeth ColorChecker[10], the Munsell set[13]), natural reflectances (the Krinov set[6] and the Westland set[19]), and Vrhel *et al.*'s Object set[17], all of which used a 10nm sampling in the range from 400nm to 700nm resulting in $q = 31$ samples. Results are shown for a linear model representation in $d = 3$ to 15 dimensions in terms of: the % variance represented by the first d principal components; mean and maximum CIE L*a*b* ΔE under an equi-energy illuminant; mean and maximum spectral error (L2 Euclidean distance from original to linear model representation).

Table (1) shows that when using 7 or more dimensions the accuracy of representation is on average below 1ΔE, using 11 and more dimensions the maximum ΔE error is also below 1 unit and with more than 14 dimensions the error is practically negligible considering any of the measures.

[1]In the presence of fluorescence, the upper bound of 1 can be redefined to a (higher) value that takes this phenomenon into account. Without loss of generality however we can assume reflectances to be less than or equal to 1.

		CIE Lab ΔE		Spectral	
d	%	μ	max	μ	max
3	0.989	5.6	63.7	0.17	0.81
4	0.994	2.8	27.4	0.12	0.70
5	0.997	2.0	22.2	0.09	0.50
6	0.998	1.0	17.1	0.07	0.33
7	0.999	0.6	10.9	0.06	0.32
8	0.999	0.5	6.0	0.04	0.28
9	1.000	0.2	4.1	0.03	0.21
10	1.000	0.1	2.2	0.03	0.20
11	1.000	0.1	0.8	0.02	0.13
12	1.000	0.1	0.9	0.02	0.11
13	1.000	0.0	0.7	0.02	0.09
14	1.000	0.0	0.4	0.01	0.07
15	1.000	0.0	0.1	0.01	0.06

Linear model representation accuracy of a set of 2086 reflectances in terms of % representation, mean and maximum CIE ΔE and mean and maximum spectral error.

Using a d-dimensional linear model representation can clearly reduce the computational complexity involved when dealing with the OCS, without necessarily compromising spectral accuracy. Thus, assuming a linear model basis in matrix $\mathbf{B}$, the OCS can be defined relative to this basis by $2q$ inequalities of $\mathbf{w}$ (in $\mathbb{R}^d$) as:

$$\begin{aligned} \mathbf{B}\mathbf{w} &\geq \mathbf{0} \\ \mathbf{B}\mathbf{w} &\leq \mathbf{1} \end{aligned} \tag{3}$$

Solving for the d dimensional OCS involves solving the half-space intersection problem defined in Eq. (3) above. This can be done using standard off–the–shelf software, such as Qhull[1]. Let us denote the OCS in $\mathbb{R}^d$ represented as a set of extreme vertices, solutions to the intersection problem in Eq. (3), as $\mathscr{O}_d$. The OCS in q-dimensions is then denoted as $\mathscr{O}_q$.

The next argument regarding $\mathscr{O}_d$ is the proportion of the OCS volume, $\mathscr{O}_q$, in $\mathbb{R}^q$ that it covers. In order to solve for the sub-set of the OCS that can be discriminated by a color input device, it is desirable for this volume to be as big as possible. Ideally of course $\mathscr{O}_d = \mathscr{O}_q$, however given the reduction in dimension necessarily some loss in volume is incurred.

In Figure 1 this volume is shown in terms of the CIE u' v' chromaticity diagram for an equi-energy illuminant. The volumes in each dimension (from 3 to 10) correspond to the OCS represented in that dimension. The basis vectors were derived using PCA of the set of 2086 surface spectral reflectances, whose dimensionality and degree of accuracy is shown in Table 1. The red dashed line represents the spectral locus and corresponds to the theoretical boundary of $\mathscr{O}_q$.

Physical realisability is a necessary condition for all surface spectral reflectances. This condition is also satisfied by highly chromatic samples which might reflect light in a very narrow range of the visible spectrum. Arguably, such samples would not occur in nature and a scanner or camera need not deal with such reflectances. However, firstly, $\mathscr{O}_d$ is represented in a space in $\mathbb{R}^d$ whose d axes are derived from actual natural reflectance samples. Thus even chromatic samples we consider are not arbitrary

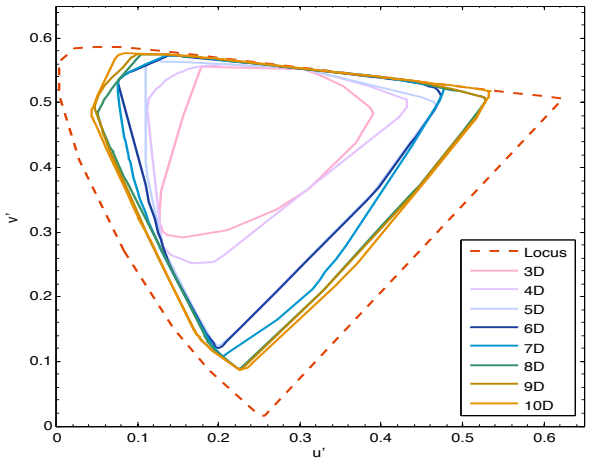

Figure 1. *CIE u' v' chromaticity diagram of $\mathcal{O}_d$ for $d = 3, \ldots, 10$ dimensions.*

but come from statistical analysis of real reflectances. Secondly, imposing further constraints (such as naturalness[4]) on surface spectral reflectances reduces the gamut of colours considerably.

Figure 2 compares the area covered by the theoretical OCS (the spectral locus), the linear model (LM) representation in $\mathcal{O}_6$ as well as a LM representation with additional *naturalness* constraints limiting surfaces to those that can be had by a convex combination of a training set (in this case the 2086 reflectances used throughout).

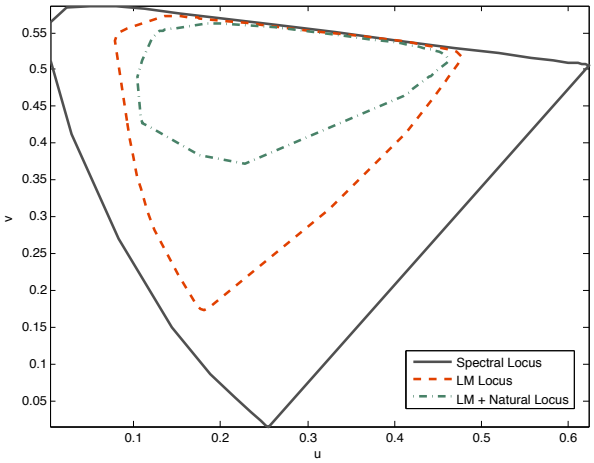

Figure 2. *CIE u' v' chromaticity diagram of theoretical spectral locus, $\mathcal{O}_6$ and $\mathcal{O}_6$ with additional natural constraints.*

Input device color acquisition model

A device response representing a Lambertian surface in a scene depends on the spectral reflectance of the surface, the illuminant spectral power distribution of the illuminating light source, the dynamic response function, repeatability and quantization bit-depth of the device. In this section, each of these contributing factors is explained in a model of device colour acquisition from reflectance to device response.

Let $\mathbf{S}$ be the $q \times c$ matrix of sensor spectral sensitivities, $\mathbf{E}$ the $q \times q$ diagonal matrix with it's diagonal elements corresponding to the illuminant spectral power distribution and $\mathbf{r}$ the $q \times 1$ spectral reflectance of a surface. To a first approximation, colour image formation can be written as:

$$\mathbf{c} = k * \mathbf{S}^T \mathbf{E} \mathbf{r} \tag{4}$$

where $\mathbf{c}$ is a $c \times 1$ vector of the device response and $k = 1/max(\mathbf{S}^T \mathbf{E} \mathbf{1})$ is a normalizing scalar constant to set $\mathbf{c} = \mathbf{1}$ for a perfect white diffuser such that $\mathbf{c} \in [0,1]$ and $*$ denotes a scalar multiplication of a matrix.

Given a linear model of surface spectral reflectance in the $q \times d$ matrix $\mathbf{B}$, from Eq. (2), Eq. (4) becomes:

$$\mathbf{c} = k * \mathbf{S}^T \mathbf{E} \mathbf{B} \mathbf{w} \tag{5}$$

where $\mathbf{w}$ is the linear model representation of reflectance $\mathbf{r}$ within $\mathbf{B}$.

Eq. (5) assumes that the response $\mathbf{c}$ is a linear correlate of surface spectral reflectance and that this response varies across the entire range of input intensities. Color input devices however commonly have non-linearities as well as clipping, both of which are described by the dynamic response function (DRF) of a device.

A DRF can be described by c $m \times 2$ matrices $\mathbf{D}_i$ $(i = 1, \ldots, c)$, one per each recording channel of a device, where m is the number of lightness levels at which a medium response's difference from the predicted response is determined. Each of the DRF matrices consists of a response modeled by Eq. (5) in it's first column, and it's corresponding actual response of the device in the second column. The surfaces used to derive matrices $\mathbf{D}_i$ are a series of m patches with near-uniform surface spectral reflectances, also referred to as achromatic or non-selective, of increasing lightness. For an actual response vector $\mathbf{c}$, the non-linearity and dynamic response of the device is accounted for by interpolating from the m values in each of the c matrices $\mathbf{D}_i$.

Since the color acquisition devices we examine are digital, the effect of quantization has to be taken into account. Devices represent the response vectors $\mathbf{c}$ with a limited number of allocated bits per channel. For a b-bit device it's range is $[0, 2^b - 1]$ on a discrete scale of integers ($[0, 255]$ for 8-bit devices, $[0, 1023]$ for 10-bit devices, etc.). This means that values that on a continuous scale of real numbers are different can, by means of quantization, become identical. The effect of quantization can be described by the following equation:

$$\mathbf{c} = round((2^b - 1) * \mathbf{c}) \tag{6}$$

where $round()$ returns the closest integer to a real number. The consequence of Eq. (6) is that the range of $\mathbf{c}$ changes from a continues, real interval $[0,1]$ to a discrete, integer interval of $[0, 2^b - 1]$.

Digital color input devices vary also from one acquisition to another. Such variation is the repeatability of a device and can be defined as a threshold value. Two reflectances that induce different responses not differing in more than the threshold value can therefore be considered as not discriminable. This criterion will be used in order to determine the boundary of the sub-set of surface spectral reflectance that can be discriminated amongst.

Device discriminability gamut calculation

Finding the sub-space of $\mathcal{O}_d$ that is distinguishable by a color input device, following the model described in the previous section, requires a sampling of this set. While the OCS in d dimensions, $\mathcal{O}_d$, is by definition a convex body (the projection of a hyper-cube), the sought sub-set need not be convex. The reason for this are the possible non-linearities in the color channels described by the dynamic response functions in the c matrices $\mathbf{D}_i$. The sampling therefore needs to be such that non-convexities can be found and represented.

The strategy chosen here is to sample $\mathcal{O}_d$ from it's centre point towards each of it's extreme vertices. The centre point for $\mathcal{O}_q$ is a non-selective reflectance that has values of 0.5 at each of it's q sampling points, denoted as $\mathbf{r}_c = 0.5 * \mathbf{1}$. Since the transform from $\mathcal{O}_q$ to $\mathcal{O}_d$ is a linear transform (defined via the $q \times d$ linear model basis matrix $\mathbf{B}$) and thus preserves Euclidean distance, also the centre point is preserved and is hence $\mathbf{w}_c = 0.5 * \mathbf{B}^T \mathbf{1}$.

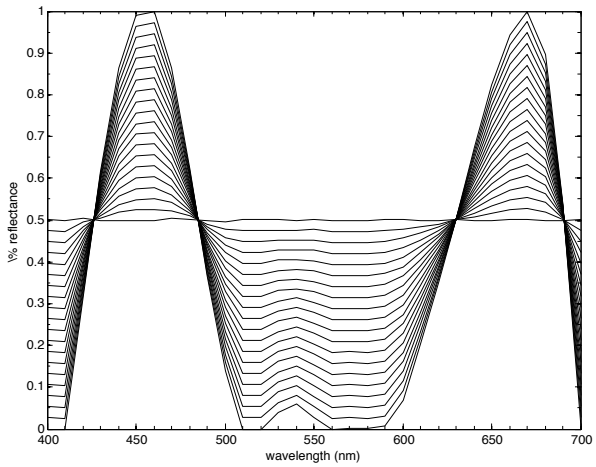

Figure 3. *An example of surface spectral reflectances corresponding to 20 linear model weights $\mathbf{w}_i$ along the line from $\mathbf{w}_c$ in $\mathcal{O}_9$.*

The algorithm proceeds as follows:

1. Each line connecting $\mathbf{w}_c$ and a point $\mathbf{w}_e$ on the convex hull of $\mathcal{O}_d$ is uniformly divided into x linear model weights $\mathbf{w}_i$ such that:

$$\mathbf{w}_i = i * \alpha * \mathbf{w}_c + i * (1 - \alpha) * \mathbf{w}_e \tag{7}$$

   whereby $\alpha = 1/(x-1)$ and $i = 1, \ldots, x$. (See Figure 3 for an example of the surface spectral reflectances corresponding to a line of $\mathbf{w}_i$)
2. The device responses to the surface spectral reflectances corresponding to the set of x linear model weights $\mathbf{w}_i$ are calculated, resulting in x response vectors $\mathbf{c}_i$.
3. For each pair of device responses $[\mathbf{c}_i, \mathbf{c}_{i+1}]$ corresponding to the line of linear model weights in step 1, their difference $d_i = |\mathbf{c}_{i+1} - \mathbf{c}_i|$ for $i = 1, \ldots, (x-1)$ is calculated, and the i for which the d_i is significant compared to the repeatability threshold value is determined.
4. The $\mathbf{w}_i$ that corresponds to the first i found in step 3 is on the boundary of the sub-space of surface spectral reflectances that the device can distinguish.

Simulation

In this section results are shown for an RGB digital camera (Agfa Studiocam[11]) and a theoretical tri-chromatic camera with sharp, narrow-band sensors with peaks at 450nm, 540nm and 610nm (the so-called prime wavelengths [2]). Their spectral sensitivities are plotted in Figure 4. The dynamic response functions (matrices $\mathbf{D}_i$, $i = 1, \ldots, 3$) of the Agfa Studiocam have been measured and are shown in Figure 5.

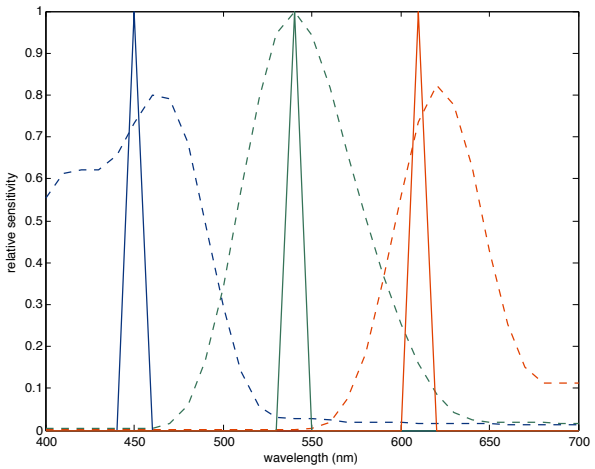

Figure 4. *The spectral sensitivities of the Agfa Studiocam RGB camera (dashed) and a theoretical tri-chromatic device with sharp, narrow-band sensors (solid).*

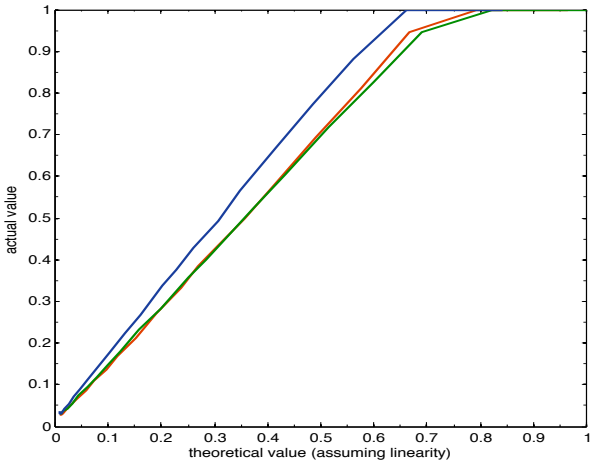

Figure 5. *The dynamic response functions of the three channels of Agfa Studiocam RGB camera.*

The sub-space of $\mathcal{O}_d$ that corresponds to the space of linear model weights $\mathbf{w}$ (which in turn correspond to surface spectral reflectances $\mathbf{r}$) that a device can distinguish is a d-dimensional polytope and as such is not straight-forward to visualize. For the purpose of this study we choose to look at the subspace of $\mathcal{O}_8$ that cannot be discriminated by plotting the CIE u'v' chromaticities of surfaces that are found to be indistinguishable by the device. In Figure 6 we plot these surfaces for both devices. It is important to note however that these plots do not represent chromaticities that

a device cannot distinguish. Instead these chromaticities are those of some (but not all) reflectances that cannot be distinguished.

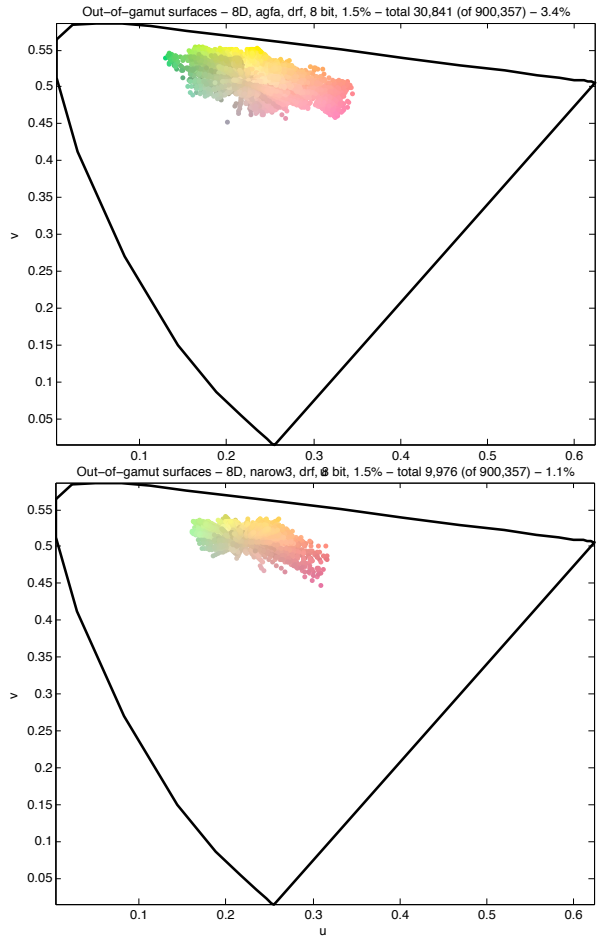

Figure 6. *Out of gamut reflectances plotted as chromaticities in CIE u'v' diagram (top - Agfa Studiocam, bottom - narrow band camera).*

$\mathscr{O}_8$ is represented by $\approx 5 \times 10^4$ vertices in $\mathbb{R}^8$. The sampling from the centre point to each of the vertices of $\mathscr{O}_8$ results in a total of $\approx 9 \times 10^5$ surface spectral reflectances examined. In the case of the Agfa Studiocam RGB camera, there are $\approx 3 \times 10^4$ reflectances that cannot be locally distinguished constituting 3.4% of the entire sampling, while in the case of the narrow band camera there are $\approx 9 \times 10^3$ reflectances undistinguishable locally, amounting to 1.1% (both sets plotted in Figure 6).

The difference in the number of out–of–gamut reflectances between the two devices gives us a *quantitative* notion of the proportion of the sampled $\mathscr{O}_8$ that cannot be distinguished by a device. While in both cases small, there are over three times as many reflectances that cannot be distinguished by the Agfa Studiocam as compared to the narrow band camera. Because of it's broad band spectral sensitivities, the Agfa Studiocam RGB camera is more prone to metamerism. Spectral variation that induces identical response in the Agfa Studiocam camera is larger than the spectral variation tolerated by a narrow band camera. In Figure 7 we calculated the set of metameric reflectances for a 50% non-selective surface's RGB response for the two cameras under illuminant D53. It can be seen that the metamer set for the Agfa Studiocam (top part of Figure 7) allows for much more spectral variation as compared to the metamer set of the narrow band camera (bottom part of Figure 7).

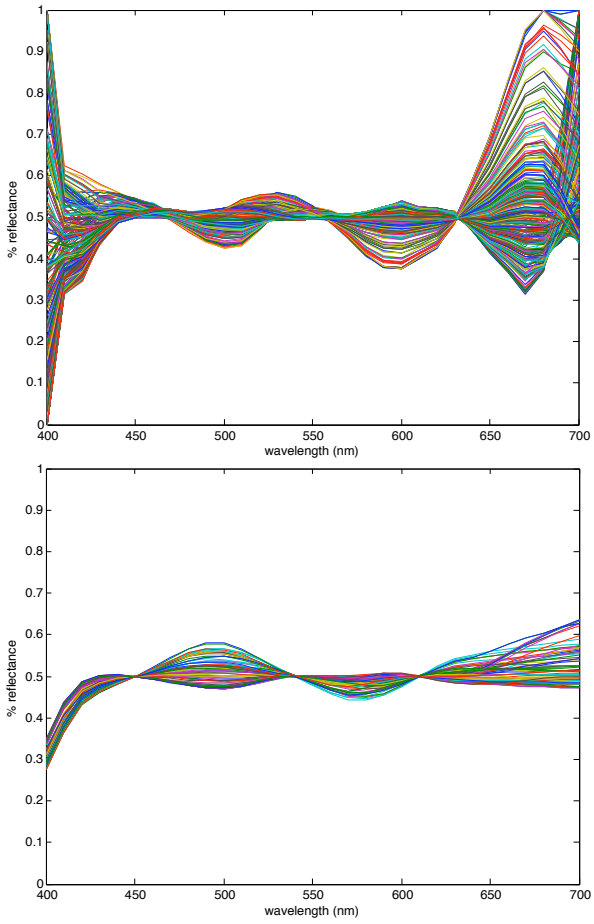

Figure 7. *Extreme reflectances inducing identical response (metamers) in the Agfa Studiocam camera (top) and the narrow band camera (bottom) corresponding to a 50% non-selective surface under illuminant D53.*

The CIE u'v' chromaticity plots on the other hand portray a *qualitative* notion of the kind of surface spectral reflectances that cannot be distinguished by the devices. Both regions correspond to areas close to the achromatic point. The reason for this is that there are many more possible surface spectral reflectances in the achromatic region than there are towards the boundary of the spectral locus[16, 12]. In the limit, surfaces that define the spectral locus are monochromatic reflectances in a unique one-to-one relation to chromaticities.

Narrow band sensors, such as those used in our experiments, have evidently advantages, however they also have many disadvantages that render them impractical. For example if one of the narrow band sensors fails, one third of the visible spectrum is not accounted for. Also, in the presence of noise, narrow band sensors would perform considerably worse, as the response is determined by variation in a single wavelength. Instead, sensors such as those of the Agfa Studiocam, having broad overlapping spectral sensi-

tivities, are better suited in both cases.

Conclusions

In this paper the problem of determining the range of surface spectral reflectances among which a color acquisition device can locally distinguish has been addressed. In order to solve this problem, the Object Color Solid has been represented in a d dimensional linear model basis. In doing so, the computational complexity of sampling a hyper-cube in $\mathbb{R}^q$ has been reduced to sampling a convex polytope in a d–dimensional subspace. The results obtained in such a way can be used for comparing the suitability of alternative sensor designs both for reflectance estimation and for general use as discriminability is a prerequisite for the former and desirable for the latter.

Acknowledgements

Peter Morovic acknowledges the Japan Society for the Promotion of Science and JSPS KAKENHI 1806703 for their financial help, as well as the support of Hideaki Haneishi (Chiba University). Jan Morovic would like to thank Virginia Palacios (Hewlett–Packard) for her support. Finally, the authors would like to thank the anonymous reviewers of the manuscript for their comments.

References

[1] C. B. Barber, D. D. Dobkin, and H. Huhdanpaa. The quickhull algorithm for convex hulls. *ACM Transactions on Mathematical Software*, 22(4):469–483, 1996.

[2] M. H. Brill, G. D. Finlayson, P. M. Hubel, and W. A. Thorntont. Prime colors and color imaging. In *IS&T/SID 6th Color Imaging Conference, Scottsdale, Arizona*, November 1998.

[3] P. D. Burns and R. S. Berns. Analysis of multispectral image capture. In *Proceedings of IS&T and SID's 4th Color Imaging Conference*, pages 19 – 22, 1996.

[4] G. D. Finlayson and P. Morovic. Metamer sets. *Journal of the Optical Society of America A*, 22:810 – 819, 2005.

[5] S. Helling. Construction of multichannel camera gamuts. In *Proceedings of Spectral Imaging: Eighth International Symposium n Multispectral Color Science, SPIE-IS&T's Electronic Imaging*, pages 1–10, 2006.

[6] E. L. Krinov. Spectral reflectance properties of natural formations. *Proc. Acad. Sci. USSR*, 1947.

[7] L. T. Maloney. Evaluation of linear models of surface spectral reflectance with small numbers of parameters. *Journal of the Optical Society of America A*, 3(10):1673–1683, October 1986.

[8] L. T. Maloney and B. A. Wandell. Color constancy: a method for recovering surface spectral reflectance. *Journal of the Optical Society of America A*, 3:29–33, 1986.

[9] D. H. Marimont and B. A. Wandell. Linear models of surface and illuminant spectra. *Journal of the Optical Society of America*, 11:1905–1913, October 1992.

[10] C. S. McCamy, H. Marcus, and J. G. Davidson. A color-rendition chart. *Journal of Applied Photographic Engineering*, 2:95 – 99, Summer 1976.

[11] J. Morovic and P. Morovic. Determining colour gamuts of digital cameras and scanners. *Color Research and Application*, 28(1):59–68, 2003.

[12] P. Morovic. *Metamer Sets*. PhD. Thesis, University of East Anglia, School of Information Systems, 2002.

[13] J. P. S. Parkkinen, J. Hallikanen, and T. Jaaskelainen. Characteristic spectra of munsell colors. *Journal of the Optical Society of America A*, 6:318–322, 1989.

[14] J. Pujol, F. Martinez-Verdu, and P. Capilla. Estimation of the device gamut of a digital camera in raw performance using optimal color-stimuli. In *Proceedings of IS&T's 2003 PICS Conference*, 2003.

[15] E. Schrödinger. Theorie der Pigmente von grösster Leuchtkraft. *Ann. Phys. (Paris)*, 62:603–622, 1920.

[16] W. S. Stiles and G. Wyszecki. Counting metameric object–color stimuli. *Journal of the Optical Society of America*, 52, 1962.

[17] M. J. Vrhel, R. Gershon, and L. S. Iwan. Measurement and analysis of object reflectance spectra. *Color Research and Application*, 19:4–9, 1994.

[18] B. A. Wandell and J. E. Farrell. Water into wine: Converting scanner rgb to tristimulus xyz. *In Device–Independent Color Imaging and Imaging Systems Integration, SPIE vol. 1909*, pages 92–101, 1993.

[19] S. Westland, J. Shaw, and H. Owens. Colour statistics of natural and man-made surfaces. *Sensor Review*, 20(1):50–55, 2000.

Author Biography

Peter Morovič received his BSc degree in theoretical computer science from the School of Mathematics and Physics at the Comenius University in Bratislava (Slovakia) and his PhD degree in computing from the School of Computing Sciences at the University of East Anglia in Norwich (UK) in 2002. Currently he is a post–doctoral research fellow at the Haneishi Laboratory of the Research Center for Frontier Medical Engineering at Chiba University (Japan).

Ján Morovič received his Ph.D. in color science from the Colour & Imaging Institute (CII) of the University of Derby (UK) in 1998, where the title of his thesis was To Develop a Universal Gamut Mapping Algorithm. After working as a lecturer in digital color reproduction at the CII he became senior color scientist at Hewlett-Packard in Barcelona, Spain. He is also the chairman of the CIEs Technical Committee 803 on Gamut Mapping.